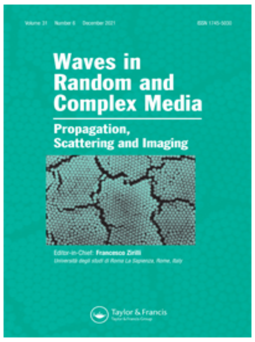

Waves in Random and Complex Media

ISSN: (Print) (Online) Journal homepage: https://www.tandfonline.com/loi/twrm20

Investigations of energy and an exchange of energies between electrostatic solitons: higher-order corrections and efficiency improvement of semiconductor plasmas

Emad Fathy EL-Shamy, Mona Mahmoud & Emad Khader El-Shewy

WAVES IN RANDOM AND COMPLEX MEDIA
2021, VOL. 31, NO. 6, 1124–1140
https://doi.org/10.1080/17455030.2019.1650987

Taylor & Francis
Taylor & Francis Group

Check for updates

Investigations of energy and an exchange of energies between electrostatic solitons: higher-order corrections and efficiency improvement of semiconductor plasmas

Emad Fathy EL-Shamy[a,b], Mona Mahmoud[c] and Emad Khader El-Shewy[d,e]

[a]Department of Physics, College of Science, King Khalid University, Abha, Kingdom of Saudi Arabia; [b]Department of Physics, Faculty of Science, Damietta University, New Damietta, Egypt; [c]Department of Physics, College of Science for Girls in Abha, King Khalid University, Abha, Kingdom of Saudi Arabia; [d]Department of Physics, Taibah University, Al-Madinah Al-Munawarrah, Saudi Arabia; [e]Theoretical Physics Research Group, Physics Department, Faculty of Science, Mansoura University, Mansoura, Egypt

ABSTRACT

Investigations of the nonlinear excitation and collisions of electrostatic solitons in a dense semiconductor plasma composed of electrons and holes are improved by using the higher-order corrections. Applying the extended Poincaré-Lighthill-Kuo (EPLK) method to obtain the Korteweg–de Vries (KdV) equations, which govern the nonlinear excitation of electrostatic solitons. Furthermore, the phase shift equations due to the collisions between electrostatic solitons are obtained. A theoretical analysis is improved by employing the KdV equations with the effects of the fifth – order dispersion terms. The numerical illustrations demonstrate that the higher-order soliton energy depends significantly on the quantum semiconductor plasma number density. On the other hand, the density of the semiconductor plasma has a weak effect on the lowest-order soliton energy. Therefore, one has to be careful about the choosing semiconductor plasma parameters to avoid any deficiency of the modern semiconductor devices.

ARTICLE HISTORY
Received 18 March 2019
Accepted 29 July 2019

1. Introduction

The study of quantum plasmas plays advanced roles in understanding the dynamics of charged carriers in semiconductor quantum devices. In particular, it is extremely interesting in nanoscale sizes of modern semiconductor electronic devices [1–4]. In general; quantum plasmas are associated with low temperatures and high densities of plasma particles unlike the classical plasmas. Over the last 20 years, scientists have made the tremendous progress in laser technologies, which give amazing opportunities to establish coherent laser sources for femtosecond pulses [5,6]. In this direction, various areas of worthy scientific research have been explored due to the interaction between powerful laser beams and quantum plasmas. Of course, in the future, new research may provide semiconductor

CONTACT Emad Fathy EL-Shamy emadel_shamy@hotmail.com

electronic devices with different new processes and high performance. Actually, the nonlinear propagation and interactions of electrostatic localized coherent waves (e.g. solitons) in semiconductor quantum plasmas play a critical role for a strong understanding of physical situations associated with semiconductor quantum devices [7–11].

It is well known that, for a semiconductor quantum plasma system, the de Broglie thermal wavelengths of the charged carriers (electrons and holes) are compared to the characteristic spatial scales of the system. Thus, a semiconductor quantum plasma model contains degenerate pressures of electrons and holes, exchange correlation potentials and the quantum recoil effects. Recently, several researchers have investigated the effects of the mentioned physical parameters on the nonlinear propagation, stabilities and collisions of solitons in quantum semiconductor plasmas [12–17]. For example, Moslem et al. [13] discussed the basic characteristics of solitons in various quantum semiconductor plasmas. They showed that the degenerate pressure has a strong effect on the reduction of the amplitude soliton. Wang et al. [14] derived the modified Schrödinger equation to examine the modulational instability of envelope solitary waves in semiconductor plasmas. They stated that the damping rate is directly proportional to the collision frequency of the electron–phonon/hole-phonon. El-Bedwehy [15] investigated the nonlinear freak wave in electron–hole quantum GaAs semiconductor plasmas. El-Bedwehy[15] demonstrated that the exchange- correlation effect has no important impact on the freak wave profile. Tolba et al. [16] used the typical values of the GaN semiconductor plasma to point out that both solitons and periodic travelling waves have negative potentials in the quantum semiconductor plasmas. Very recently, El-Shamy et al. [17] illustrated that the variation in the studied system's geometry plays a vital role in the properties of the dark solitary pulses. However, most of the previous work was limited to the study of the nonlinear excitation and collisions, by obtaining the Korteweg–de Vries (KdV) equations and their phase shift equations, for small amplitudes of electrostatic solitons in an electron–hole semiconductor plasma regime. In effect, by increasing the amplitude soliton, both the velocity and width of a solitary wave deviate from the prediction of the well-known KdV equation (i.e. the KdV equation breaks down) [18]. Therefore, to overcome this weakness, the fifth-order dispersion terms are added to the evolution equations, which govern the nonlinear propagation of solitons. In other words, to obtain better predictions of the reductive perturbation method, an adopted technique is used to get the higher-order soliton solutions, and hence the higher-order phase shifts are deduced [18–25]. Thus, the KdV equations with fifth-order dispersion terms are used and higher-order electrostatic soliton solutions and then the higher-order phase shifts are obtained. Very recently, by using the extended Poincaré-Lighthill-Kuo (EPLK) method [26–28] and the higher-order corrections [24,29], EL-Shamy et al. [30] examined the face-to-face collision of dust ion acoustic solitons in weakly relativistic dusty plasmas with superthermality. They illustrated that the higher-order phase shift is highly sensitive in comparison to the lowest-order phase shift. Consequently, our objective is to discuss the effects of the higher-order corrections on the excitation and face-to-face collisions of electrostatic solitons in dens semiconductor plasmas.

The paper is organized as follows: In Section 2, the basic model is given. Furthermore, by using the EPLK perturbation method, the KdV equations and the phase shifts are obtained. In Section 3, the higher-order corrections of the nonlinear excitation and collisions of electrostatic solitons are discussed. The lowest-order and the higher-order correction of the electrostatic soliton energies are determined in Section 4. Section 5 is dedicated to numerical investigations, the general discussion and conclusion.

2. Governing equations

Using the quantum hydrodynamic (QHD) model, the governing equations for an electron-hole semiconductor quantum plasma are written as [15–17].

$$\frac{\partial n_{e,h}}{\partial t}+\frac{\partial (n_{e,h}u_{e,h})}{\partial x}=0, \tag{1}$$

$$\frac{\partial u_{e,h}}{\partial t}+u_{e,h}\frac{\partial u_{e,h}}{\partial x}\pm \mu_{e,h}\frac{\partial \phi}{\partial x}+\gamma_{e,h}\frac{\partial V_{xce,h}}{\partial x}+\sigma_{e,h}n_{e,h}^{-1/3}\frac{\partial n_{e,h}}{\partial x} - 2H_{e,h}^{2}\frac{\partial}{\partial x}\left(\frac{\frac{\partial^2}{\partial x^2}\sqrt{n_{e,h}}}{\sqrt{n_{e,h}}}\right)=0, \tag{2}$$

$$\frac{\partial^2 \phi}{\partial x^2}=n_e-n_h. \tag{3}$$

Here, the physical quantities n_e (n_h) and u_e (u_h) are, respectively, the density and the velocity of electrons (holes). ϕ is the electrostatic potential. In Equation (2), on the left-hand side, the fourth term is the exchange - correlation force between the identical particles when their wave functions overlap because of the high number density of the electrons and holes, the fifth term is the degenerate pressure due to the high number density of the electrons and holes, and the last term is the quantum recoil force associated with the Bohm potential due to the electrons/holes tunneling through a potential barrier. At equilibrium, we have $n_{e0}=n_{h0}=n_0$, where n_{e0} (n_{h0}) is the unperturbed electron (hole) density and n_0 is a common density. Here, the exchange - correlation potential for electrons (holes) is written as [13]

$$V_{xce(h)}\left(=0.985(e^2/\epsilon)n_{e(h)}^{1/3}\left[1+\left(0.034/a^{*}_{Be(h)}n_{e(h)}^{1/3}\right)\ln\left(1+18.376a^{*}_{Be(h)}n_{e(h)}^{1/3}\right)\right]\right),$$

where $a^{*}_{Be}=\epsilon\hbar^2/m_e^{*}e^2$($a^{*}_{Bh}=\epsilon\hbar^2/m_h^{*}e^2$) is the effective Bohr radius for electrons(holes), ϵ is the dielectric constant of the material, $m_e^{*}(m_h^{*})$ is the effective mass of electron(hole), $\hbar=h/2\pi$, where h is Planck constant, and e is the magnitude of the electron charge. $\mu_e(=1)$, $\gamma_e(=1/k_BT_{Fe})$, $\sigma_e(=(\pi/3)^{1/3}(\pi\hbar^2/2m_e^{*})(n_{e0}^{2/3}/k_BT_{Fe}))$ and $H_e(=\hbar\omega_{pe}/2k_BT_{Fe})$ for electrons and $\mu_h(=\mu=m_e^{*}/m_h^{*})$, $\gamma_h(=\mu/k_BT_{Fh})$, $\sigma_h(=(\pi/3)^{1/3}(\pi\hbar^2/2m_h^{*})(n_{h0}^{2/3}/k_B T_{Fh})\mu)$ and $H_h(=\mu\hbar\omega_{ph}/2k_BT_{Fh})$ for holes, where $\omega_{pe}(\omega_{ph})$ is the electron (hole) frequency, and k_B is Boltzmann constant. $n_{e,h}, u_{e,h}, \phi$, x, and t are, respectively, scaled by $n_{e0,h0}$, $V_{Fe}(=\sqrt{k_BT_{Fe}/m_e^{*}})$, k_BT_{Fe}/e, $\lambda_{DFe}(=\sqrt{k_BT_{Fe}/4\pi e^2 n_{e0}})$, and $\omega_{pe}^{-1}(=\sqrt{m_e^{*}/4\pi e^2 n_{e0}})$. V_{Fe} is the Fermi electron thermal speed, λ_{DFe} is the Fermi electron Debye radius, and $T_{Fe(h)}(=(\hbar^2/2m^{*}_{e(h)}k_B)(3\pi^2 n_{e(h)0})^{2/3})$ is the electron (hole) Fermi temperature in the non-relativistic and zero-temperature limits.

Now, let us examine the face-to-face collision between electrostatic solitons. We apply the well-known the EPLK method to obtain the KdV equations [31–34]. The dependent variables are expanded as follows:

$$\mathrm{Y} = \mathrm{Y}^{(0)} + \sum_{n=1}^{\infty} \varepsilon^{(n+1)} \mathrm{Y}^{(n)}, \tag{4}$$

where $\mathrm{Y} = [n_e, n_h, u_e, u_h, \phi]$, and $\mathrm{Y}^{(0)} = [1\ ,\ 1,\ 0,\ 0, 0]$. Furthermore, the independent variables are stretched as

$$\begin{aligned} \xi &= \varepsilon(\mathrm{x} - \lambda t) + \varepsilon^2 \mathrm{P}^{(0)}(\zeta, \tau) + \ldots, \\ \zeta &= \varepsilon(\mathrm{x} + \lambda t) + \varepsilon^2 \mathrm{Q}^{(0)}(\xi, \tau) + \ldots, \\ \tau &= \varepsilon^3 \mathrm{t}, \end{aligned} \tag{5}$$

where ε is a smallness parameter, which is used to measure the weakness of the nonlinearity, and λ is the wave velocity. Substituting Equations (4) and (5) into Equations (1) – (3), considering the lowest nonzero order in ε, we obtain the following relations:

$$\mathrm{n}_{\mathrm{e}}^{(1)} = \frac{-1}{(\lambda^2 - \ \chi_{\mathrm{e}})}(\phi_1^{(1)}(\xi, \tau) + \phi_2^{(1)}(\zeta, \tau)), \tag{6}$$

$$\mathrm{n}_{\mathrm{h}}^{(1)} = \frac{\mu}{(\lambda^2 - \chi_{\mathrm{h}})}(\phi_1^{(1)}(\xi, \tau) + \phi_2^{(1)}(\zeta, \tau)) \tag{7}$$

$$\mathrm{u}_{\mathrm{e}}^{(1)} = \frac{-\lambda}{(\lambda^2 - \ \chi_{\mathrm{e}})}(\phi_1^{(1)}(\xi, \tau) - \phi_2^{(1)}(\zeta, \tau)) \tag{8}$$

$$\mathrm{u}_{\mathrm{h}}^{(1)} = \frac{\mu\lambda}{(\lambda^2 - \chi_{\mathrm{h}})}(\phi_1^{(1)}(\xi, \tau) - \phi_2^{(1)}(\zeta, \tau)) \tag{9}$$

where $\chi_{\mathrm{e}}(= \alpha_{\mathrm{e}} + \beta_{\mathrm{e}} + \sigma_{\mathrm{e}})$, $\chi_{\mathrm{h}}(= \alpha_{\mathrm{h}} + \beta_{\mathrm{h}} + \sigma_{\mathrm{h}})$, $\alpha_{\mathrm{e}}(= \alpha_{1\mathrm{e}}/3\mathrm{k_B T_{Fe}})$, $\beta_{\mathrm{e}}(= \beta_{1\mathrm{e}}\beta_{2\mathrm{e}}/\mathrm{k_B T_{Fe}})$, $\alpha_{\mathrm{h}}(= \alpha_{1\mathrm{h}}/3\mathrm{k_B T_{Fe}})$, $\beta_{\mathrm{h}}(= \mu\beta_{1\mathrm{h}}\beta_{2\mathrm{h}}/\mathrm{k_B T_{Fe}})$, $\alpha_{1\mathrm{e}} = 0.985(e^2/\epsilon)\mathrm{n}_0^{1/3}$, $\beta_{1\mathrm{e}} = 0.985\mathrm{x}0.034\ (e^2/\epsilon \mathrm{a}_{\mathrm{Be}}^*)$, $\beta_{2\mathrm{e}} = \frac{1}{3}(18.37\ \mathrm{a}_{\mathrm{Be}}^* \mathrm{n}_0^{1/3}/(1 + 18.37\ \mathrm{a}_{\mathrm{Be}}^* \mathrm{n}_0^{1/3}))$, $\alpha_{1\mathrm{h}} = \mu\alpha_{1\mathrm{e}}$, $\beta_{1\mathrm{h}} = 0.985\mathrm{x}0.034\ (e^2/\epsilon \mathrm{a}_{\mathrm{Bh}}^*)$ and $\beta_{2\mathrm{h}} = \frac{1}{3}(18.37\ \mathrm{a}_{\mathrm{Bh}}^* \mathrm{n}_0^{1/3}/(1 + 18.37\ \mathrm{a}_{\mathrm{Bh}}^* \mathrm{n}_0^{1/3}))$.

Therefore, for the lowest nonzero order in ε of the Poisson equation, one can obtain the following wave velocity: $\lambda = \sqrt{(\mu\chi_{\mathrm{e}} + \chi_{\mathrm{h}})/(1 + \mu)}$. Moreover, in the next higher-order of ε, we can arrive at the following KdV equations:

$$\frac{\partial \phi_1^{(1)}}{\partial \tau} + \mathrm{A}\phi_1^{(1)} \frac{\partial \phi_1^{(1)}}{\partial \xi} + \mathrm{B}\frac{\partial^3 \phi_1^{(1)}}{\partial \xi^3} = 0, \tag{10}$$

$$\frac{\partial \phi_2^{(1)}}{\partial \tau} - \mathrm{A}\phi_1^{(1)} \frac{\partial \phi_2^{(1)}}{\partial \zeta} - \mathrm{B}\frac{\partial^3 \phi_2^{(1)}}{\partial \zeta^3} = 0, \tag{11}$$

$$\frac{\partial \mathrm{P}^{(0)}}{\partial \zeta} = -\frac{\mathrm{C}}{2}\phi_2^{(1)}, \tag{12}$$

$$\frac{\partial \mathrm{Q}^{(0)}}{\partial \xi} = -\frac{\mathrm{C}}{2}\phi_1^{(1)}. \tag{13}$$

where A is the nonlinearity coefficient and B is the dispersion coefficient. The coefficients A, B and C can be written as

$$A = \frac{\frac{(3\lambda^2-(2\chi_h/3)-\rho_h)\mu^2}{(\lambda^2-\chi_h)^3} - \frac{(3\lambda^2-(2\chi_e/3)-\rho_e)}{(\lambda^2-\chi_e)^3}}{(2\lambda/(\lambda^2-\chi_e)^2)+(2\mu\lambda/(\lambda^2-\chi_h)^2)}, \tag{14}$$

$$B = \frac{[1-(H_e^2/(\lambda^2-\chi_e)^2)-(\mu H_h^2/(\lambda^2-\chi_h)^2)]}{(2\lambda/(\lambda^2-\chi_e)^2)+(2\mu\lambda/(\lambda^2-\chi_h)^2)}, \tag{15}$$

$$C = \frac{\frac{(\lambda^2+(2\chi_h/3)+\rho_h)}{(\lambda^2-\chi_h)^3} - \frac{(\lambda^2+(2\chi_e/3)+\rho_e)}{(\lambda^2-\chi_e)^3}}{(2\lambda/(\lambda^2-\chi_e)^2)+(2\mu\lambda/(\lambda^2-\chi_h)^2)}, \tag{16}$$

where, $\rho_e = -(\sigma_e/3) + \beta_e\beta_{2e}$, and $\rho_h = -(\sigma_h/3) + \beta_h\beta_{2h}$.

Let us consider $\phi_1^{(1)} = \Phi_1$, and $\phi_2^{(1)} = \Phi_2$. The single-pulse soliton solutions of Equations (10) and (11)and the corresponding phase shifts are, respectively, written as

$$\Phi_1 = \psi_1 \mathrm{sech}^2\left[\left(\frac{A\psi_1}{12B}\right)^{1/2}\left(\xi - \frac{1}{3}A\psi_1\tau\right)\right], \tag{17}$$

$$\Phi_2 = \psi_2 \mathrm{sech}^2\left[\left(\frac{A\psi_2}{12B}\right)^{1/2}\left(\zeta + \frac{1}{3}A\psi_2\tau\right)\right], \tag{18}$$

$$\Delta P = \varepsilon^2 C\left(\frac{12B\psi_2}{A}\right)^{1/2}, \tag{19}$$

$$\Delta Q = -\varepsilon^2 C\left(\frac{12B\psi_1}{A}\right)^{1/2}. \tag{20}$$

where ψ_1 and ψ_2 are the amplitudes of two electrostatic solitons. Equations (10) and (11) govern the excitation of electrostatic solitons for small and finite amplitudes. Evidently, the main observations of the experimental data were demonstrated that the lowest-order soliton solutions despised the soliton amplitude by as extremely as 20% [35,36]. Therefore, the basic features (such as amplitudes, widths, and velocities) may deviate from those experimental results obtained. At this point, studying the nonlinear propagation of electrostatic solitons based on the higher-order correction would be very instructive.

3. Effects of the higher-order corrections on the nonlinear excitation and collisions

Now let us investigate the impacts of higher-order corrections on the nonlinear excitation and collisions of electrostatic solitons in dens semiconductor plasmas. Using the higher-order corrections, which is a confirmed powerful method [18,19,30]. Therefore, the KdV equations with the fifth – order dispersion terms are applied [18,19,30]

$$\frac{\partial\Phi_1}{\partial\tau} + A\Phi_1\frac{\partial\Phi_1}{\partial\xi} + B\frac{\partial^3\Phi_1}{\partial\xi^3} + \varepsilon\frac{\partial^5\Phi_1}{\partial\xi^5} = 0, \tag{21}$$

$$\frac{\partial\Phi_2}{\partial\tau} - A\Phi_2\frac{\partial\Phi_2}{\partial\zeta} - B\frac{\partial^3\Phi_2}{\partial\zeta^3} - \varepsilon\frac{\partial^5\Phi_2}{\partial\zeta^5} = 0, \tag{22}$$

In general, the higher-order equations are well known and are often contained secular terms. Equations (21) and (22) clearly contain the higher-order dispersion terms. Consequently, we cannot obtain the exact solutions of Equations (21) and (22). On the other hand, the higher-order soliton solutions are obtained by using a perturbation technique, which depends mainly on a soliton velocity correction to eliminate the secular terms. Therefore, the independent variables are given by [18,19,30].

$$\Xi = \xi - \Lambda\tau, \tag{23}$$

$$Z = \zeta + \Lambda\tau. \tag{24}$$

We can substitute Equations (23) and (24) into Equations (21) and (22), respectively.

$$-\Lambda\frac{d\Phi_1}{d\Xi} + A\Phi_1\frac{d\Phi_1}{d\Xi} + B\frac{d^3\Phi_1}{d\Xi^3} + \varepsilon\frac{d^5\Phi_1}{d\Xi^5} = 0, \tag{25}$$

$$-\Lambda\frac{d\Phi_2}{dZ} + A\Phi_2\frac{d\Phi_2}{dZ} + B\frac{d^3\Phi_2}{dZ^3} + \varepsilon\frac{d^5\Phi_2}{dZ^5} = 0. \tag{26}$$

Using the perturbation technique, the variables $\Phi_1(\Xi)$, $\Phi_2(Z)$ and Λ are expanded as follows:

$$\Phi_1 = \Phi_{01} + \varepsilon\Phi_{11} + \varepsilon^2\Phi_{21} + \ldots, \tag{27}$$

$$\Phi_2 = \Phi_{02} + \varepsilon\Phi_{12} + \varepsilon^2\Phi_{22} + \ldots, \tag{28}$$

$$\Lambda = \Lambda_0 + \varepsilon\Lambda_1 + \varepsilon^2\Lambda_2 + \ldots. \tag{29}$$

The resulting equations depend on the order of ε . Details are given in Appendix. By applying the boundary conditions (i.e. Φ_{i1}, Φ_{i2}, $\frac{d\Phi_{i1}}{d\Xi}$, $\frac{d\Phi_{i2}}{dZ}$, $\frac{d^2\Phi_{i1}}{d\Xi^2}$ and $\frac{d^2\Phi_{i2}}{dZ^2}$ ($i = 0,1,2, \ldots$), which vanish at both Ξ and $Z = \pm\infty$). For ε^0, the electrostatic soliton solutions are written as:

$$\Phi_{01} = \psi_{m0}\text{sech}^2(D\Xi), \tag{30}$$

$$\Phi_{02} = \psi_{m0}\text{sech}^2(DZ), \tag{31}$$

where $\psi_{m0}(= 3\Lambda_0/A)$ and $D^{-1}\left(= \sqrt{12B/A\psi_{m0}}\right)$ are the amplitude and the width of the electrostatic soliton. In the first-order (i.e., ε^1), after a bit of manipulation, we arrive at

$$\begin{aligned} L_\Xi\Phi_{11} = {} & (3(A\psi_{m0}/3)^{3/2}(-\Lambda_1 + (A\psi_{m0}/3)^2)\text{sech}^2(D\Xi) \\ & + (A\psi_{m0}/3)^{7/2}(-45\text{sech}^4(D\Xi) + 67.5\,\text{sech}^6(D\Xi)))\tanh(D\Xi), \end{aligned} \tag{32}$$

$$\begin{aligned} L_Z\Phi_{12} = {} & (3(A\psi_{m0}/3)^{3/2}(-\Lambda_1 + (A\psi_{m0}/3)^2)\text{sech}^2(DZ) \\ & + (A\psi_{m0}/3)^{7/2}(-45\text{sech}^4(DZ) + 67.5\,\text{sech}^6(DZ)))\tanh(DZ). \end{aligned} \tag{33}$$

where the operators L_Ξ and L_Z are written as

$$L_\Xi = -\Lambda_0\frac{d}{d\Xi} + A\frac{d\Phi_{01}}{d\Xi} + B\frac{d^3}{d\Xi^3}, \tag{34}$$

$$L_Z = -\Lambda_0\frac{d}{dZ} + A\frac{d\Phi_{02}}{dZ} + B\frac{d^3}{dZ^3}. \tag{35}$$

It is worth noticing that the operators L_{Ξ} and L_Z include the first-order and the third-order derivatives. Equations (32) and (33) are the inhomogeneous third-order linear differential equations with respect to Φ_{11} and Φ_{12}, respectively. The homogeneous equations, $L_{\Xi}\Phi_{11} = 0$ and $L_Z\Phi_{12} = 0$, are well known to possess the solutions that proportional to $\text{sech}^2(D\Xi)\tanh(D\Xi)$ and $\text{sech}^2(DZ)\tanh(DZ)$, respectively. Therefore, the existence of the terms $\text{sech}^2(D\Xi)\tanh(D\Xi)$ and $\text{sech}^2(DZ)\tanh(DZ)$ in the inhomogeneous terms on the right-hand side of Equations (32) and (33), respectively, leads to the secularity. In other words, the right-hand sides of Equations (32) and (33) have secular terms. In order to remove the secular terms, we can put the coefficients of $\text{sech}^2(D\Xi)\tanh(D\Xi)$ and $\text{sech}^2(DZ)\tanh(DZ)$ to zero. Thus, we obtain the following relation.

$$\Lambda_1 = (A\psi_{m0}/3)^2 \tag{36}$$

The solutions of the inhomogeneous equations (i.e. Equations (32) and (33)) without secularities are given by

$$\Phi_{11} = (A\psi_{m0})^2(-0.8333\,\text{sech}^2(D\Xi) + 1.250\,\text{sech}^4(D\Xi)), \tag{37}$$

$$\Phi_{12} = (A\psi_{m0})^2(-0.8333\,\text{sech}^2(DZ) + 1.250\,\text{sech}^4(DZ)). \tag{38}$$

Applying the same strategy, we can proceed to higher-order equations

$$\Lambda_2 = 0, \tag{39}$$

$$\Phi_{21} = (A\psi_{m0})^3(0.208\text{sech}^2(D\Xi) - 3.229\text{sech}^4(D\Xi) + 3.229\text{sech}^6(D\Xi)), \tag{40}$$

$$\Phi_{22} = (A\psi_{m0})^3(0.208\,\text{sech}^2(DZ) - 3.229\,\text{sech}^4(DZ) + 3.229\,\text{sech}^6(DZ)). \tag{41}$$

Now, we can combine Equations (32),(33),(36),(37),(38), (40) and (41) into Equations (23),(24), (27), (28) and (29) to obtain the higher-order soliton solutions of the KdV equations with fifth-order dispersion terms [18,19,26]. For simplicity, let us consider $\Phi_1 = \Phi_{1h}$, and $\Phi_2 = \Phi_{2h}$.

$$\Phi_{1h}(\xi,\tau) = \psi_1[\alpha_1 + \beta_1\varepsilon\psi_1\text{sech}^2(\Theta_1) + \gamma(\varepsilon\psi_1)^2\text{sech}^4(\Theta_1)]\text{sech}^2(\Theta_1), \tag{42}$$

$$\Phi_{2h}(\zeta,\tau) = \psi_2[\alpha_2 + \beta_2\varepsilon\psi_2\text{sech}^2(\Theta_2) + \gamma(\varepsilon\psi_2)^2\text{sech}^4(\Theta_2)]\text{sech}^2(\Theta_2), \tag{43}$$

where

$$\alpha_{1,2} = \left(1 - \varepsilon\left(0.833\frac{A\,\psi_{1,2}}{B^2}\right) + \varepsilon^2\left(0.208\left(\frac{A\,\psi_{1,2}}{B^2}\right)^2\right)\right), \beta_{1,2} = \left(1.250\frac{A}{B^2} - \varepsilon\psi_{1,2}\gamma\right),$$

$$\gamma = 3.320\left(\frac{A}{B^2}\right)^2 \Theta_1 = \left(\frac{A\psi_1}{12B}\right)^{1/2}\left(\xi - \frac{1}{3}A\psi_1\left(1 - \varepsilon\left(\frac{A\psi_1}{3B^2}\right)\right)\tau\right), \text{ and}$$

$$\Theta_2 = \left(\frac{A\psi_2}{12B}\right)^{1/2}\left(\zeta + \frac{1}{3}A\psi_2\left(1 - \varepsilon\left(\frac{A\psi_2}{3B^2}\right)\right)\tau\right).$$

Substituting Equations (42) and (43) into Equations (13) and (14), and after some algebraic manipulation, the higher-order leading phase shifts are written as [30].

$$P_h^{(0)} = \frac{C}{2}\left(\frac{A\psi_2}{12B}\right)^{-1/2}[K_1 + K_2\tanh(\Theta_2) + K_3\tanh^3(\Theta_2) + K_4\text{sech}^4(\Theta_2) + K_5\text{sech}^4(\Theta_2)\tanh^2(\Theta_2)], \quad (44)$$

$$Q_h^{(0)} = \frac{C}{2}\left(\frac{A\psi_1}{12B}\right)^{-1/2}[N_1 + N_2\tanh(\Theta_1) + N_3\tanh^3(\Theta_1) + N_4\text{sech}^4(\Theta_1) + N_5\text{sech}^4(\Theta_1)\tanh^2(\Theta_1)], \quad (45)$$

where

$$K_1 = \psi_2(\alpha_2 + 0.666\varepsilon\psi_2\,\beta_2 + 0.533(\varepsilon\psi_2)^2\gamma),$$
$$K_2 = \psi_2(\alpha_2 + \varepsilon\psi_2\,\beta_2 + 0.533(\varepsilon\psi_2)^2\gamma),$$
$$K_3 = -0.333\varepsilon(\psi_2)^2\beta_2,$$
$$K_4 = 0.466\varepsilon^2(\psi_2)^3\gamma \text{ and}$$
$$K_5 = -0.2\varepsilon^2(\psi_2)^3\gamma,$$
$$N_1 = \psi_1(\alpha_1 + 0.666\varepsilon\psi_1\beta_1 + 0.533(\varepsilon\psi_1)^2\gamma),$$
$$N_2 = \psi_1(\alpha_1 + \varepsilon\psi_1\beta_1 + 0.533(\varepsilon\psi_1)^2\gamma),$$
$$N_3 = -0.333\varepsilon(\psi_1)^2\beta_1,$$
$$N_4 = 0.466\varepsilon^2(\psi_1)^3\gamma \text{ and}$$
$$N_5 = -0.2\varepsilon^2(\psi_1)^3\gamma.$$

Accordingly, the higher-order phase shifts are given by [30].

$$\Delta P_h = \varepsilon^2\frac{2\sqrt{3}C\left(B^4 - \frac{2}{9}^2A^2\psi_2^2\right)}{B^{7/2}\sqrt{A\psi_2}} = \Delta P\left(1 - 0.222^2\left(\frac{A\psi_2}{B^2}\right)^2\right), \quad (46)$$

$$\Delta Q_h = -\varepsilon^2\frac{2\sqrt{3}C\left(B^4 - \frac{2}{9}^2A^2\psi_1^2\right)}{B^{7/2}\sqrt{A\psi_1}} = -\Delta Q\left(1 - 0.222^2\left(\frac{A\psi_1}{B^2}\right)^2\right). \quad (47)$$

4. The electrostatic soliton energy

A nonlinear medium, such as plasma, famously admits solitary wave solutions. Of course, this happens due to the balance between nonlinear and dispersive effects of the medium. The studies of a soliton energy in a nonlinear medium are well known to provide a powerful way to investigate the soliton in plasma. Accordingly, it is instructive at this point to consider not only the amplitude and trajectory of the electrostatic soliton but also on the lowest-order and the higher-order electrostatic soliton energies. Clearly, the soliton amplitude is the main physical parameter that we employ to obtain the soliton energy. Therefore, the soliton energy is written as [37,38]:

$$E_j = \int_{-\infty}^{\infty} \Phi_i^2(\varsigma)d\varsigma, \tag{48}$$

where the subscript 'j' refers to 1S and 2S (1H and 2H) in the lowest (higher)-order (correction). Moreover, the subscript 'i' refers to 1 and 2 in the lowest-order, and 1 h and 2 h in the higher-order correction. Obviously, we have two solitons, one of which, $\Phi_{1,1h}$, is traveling to the right (i.e., $\varsigma = \Xi$), and the other one, $\Phi_{2,2h}$, is going to the left (i.e., $\varsigma = Z$). On one hand, after performing the integral in Equations (48), by containing the lowest-order soliton solutions in Equations (17) and (18), one can obtain the lowest-order electrostatic soliton energy

$$E_{1S,2S} = \frac{4}{3}\,\text{x widt x (amplitude)}^2 = 4.62\left(\frac{B\psi_{1,2}^3}{A}\right)^{1/2}, \tag{49}$$

On the other hand, we can integrate Equation (48) by including the higher-order soliton solutions Φ_{1h} and Φ_{2h} (i.e. Equations (42) and (43), respectively). Thus the higher-order electrostatic soliton energy is given by

$$E_{1H,2H} = 13.8564\left(\frac{B\psi_{1,2}^3}{A}\right)^{1/2} \times \begin{bmatrix} 0.3333\alpha_{1,2}^2 + 0.0533\alpha_{1,2}\beta_{1,2}\psi_{1,2} + 0.0045\alpha_{1,2}\gamma(\psi_{1,2})^2 \\ +0.0022(\beta_{1,2}\psi_{1,2})^2 + 0.0004\beta_{1,2}\gamma(\psi_{1,2})^3 + 0.0001(\gamma\psi_{1,2}^2)^2 \end{bmatrix}. \tag{50}$$

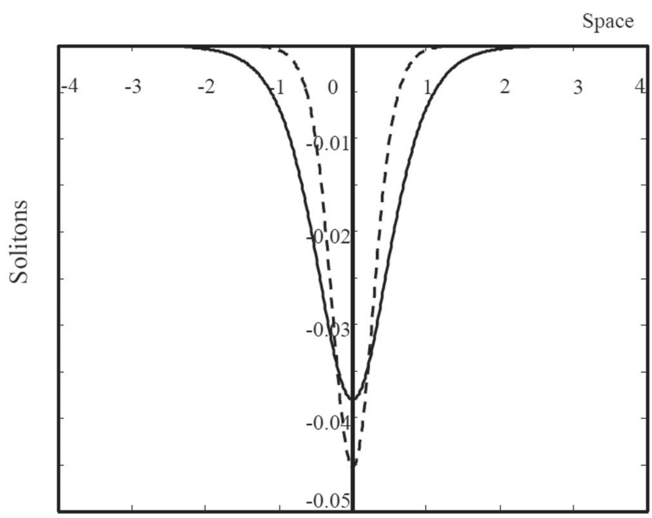

Figure 1. The lowest-order soliton (solid curve) and the higher-order soliton (dashed curve) for GaAs semiconductor.

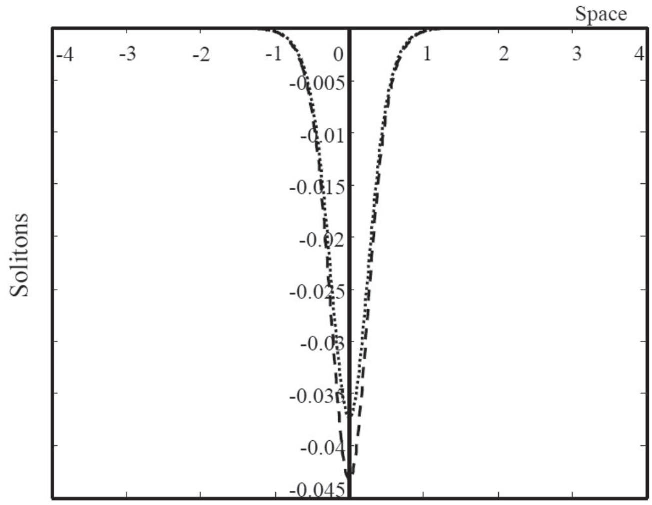

Figure 2. The higher-order soliton for GaAs semiconductor with $n_0 = 10^{16}$ cm^{-3} (dashed curve) and $n_0 = 10^{17}$ cm^{-3} (dotted curve).

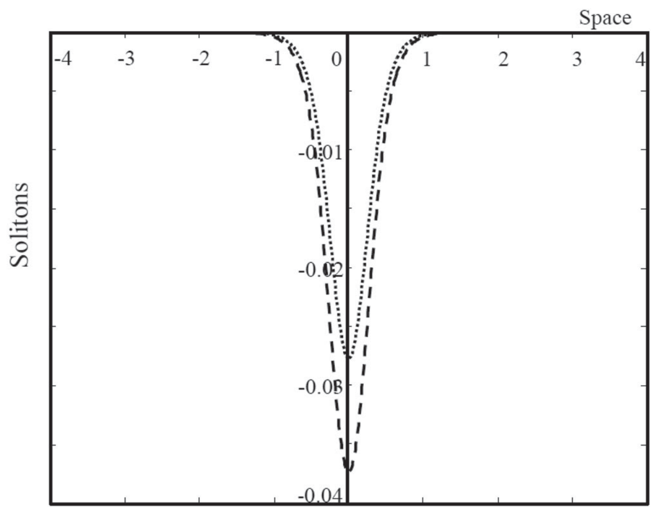

Figure 3. The higher-order soliton for GaAs semiconductor in the presence of $V_{xce,h}$ (dashed curve) and in the absence of $V_{xce,h}$ (dotted curve).

5. Numerical investigations and discussion

In this work, we have improved the theoretical investigation by studying the influences of higher-order corrections on the nonlinear excitation and collisions of electrostatic solitons in dens semiconductor plasmas. Consequently, soliton and higher-order soliton solutions and phase shifts and higher-order phase shifts have been examined for various physical parameters in GaAs semiconductors [8,9,17,39] by using $\varepsilon = 0.1$ and $\psi_1 = -0.05$. In detail, the effects of the mentioned different physical terms are discussed in the following

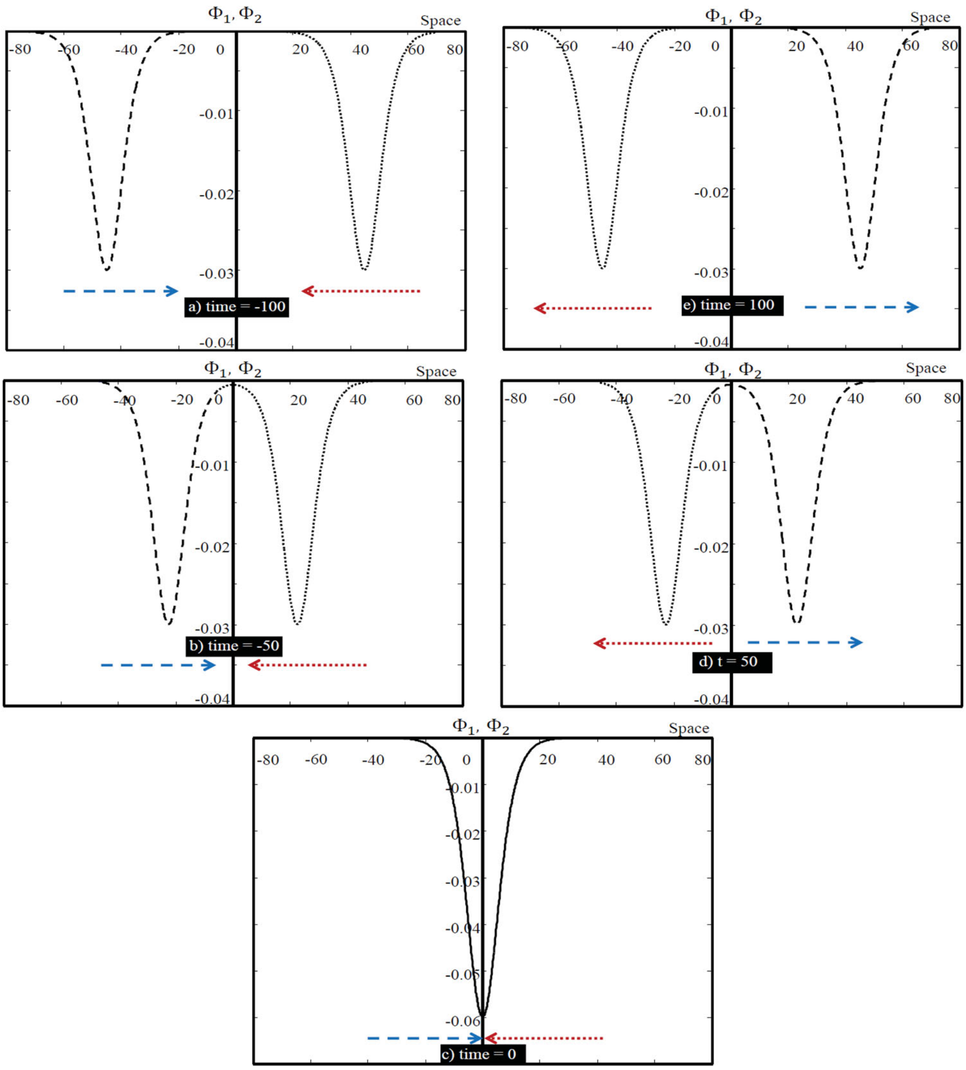

Figure 4. The face-to-face collision profiles between two lowest-order electrostatic solitons for GaAs semiconductor at different times.

Figures: Figure 1 shows the lowest-order and the higher-order electrostatic solitons as a function of space. It is obvious that the inclusion of higher-order dispersion term causes an increase in the negative electrostatic soliton amplitude. In other words, of interest is to note that in the higher-order correction, the electrostatic soliton has more amplitude by as extremely as 20%. Therefore, the fact that cannot be ignored is that the lowest-order electrostatic solitons may not only be a real case in semiconductor plasmas, but that the higher-order electrostatic solitons may also be more realistic in quantum semiconductor plasmas. Figure 2 presents the waveform of the electrostatic soliton in the higher-order correction for different values of the quantum semiconductor plasma number density n_0. The electrostatic soliton waveform increases with the decrease of the quantum semiconductor plasma number density n_0. Figure 3 examines the effect of the presence/the absence of

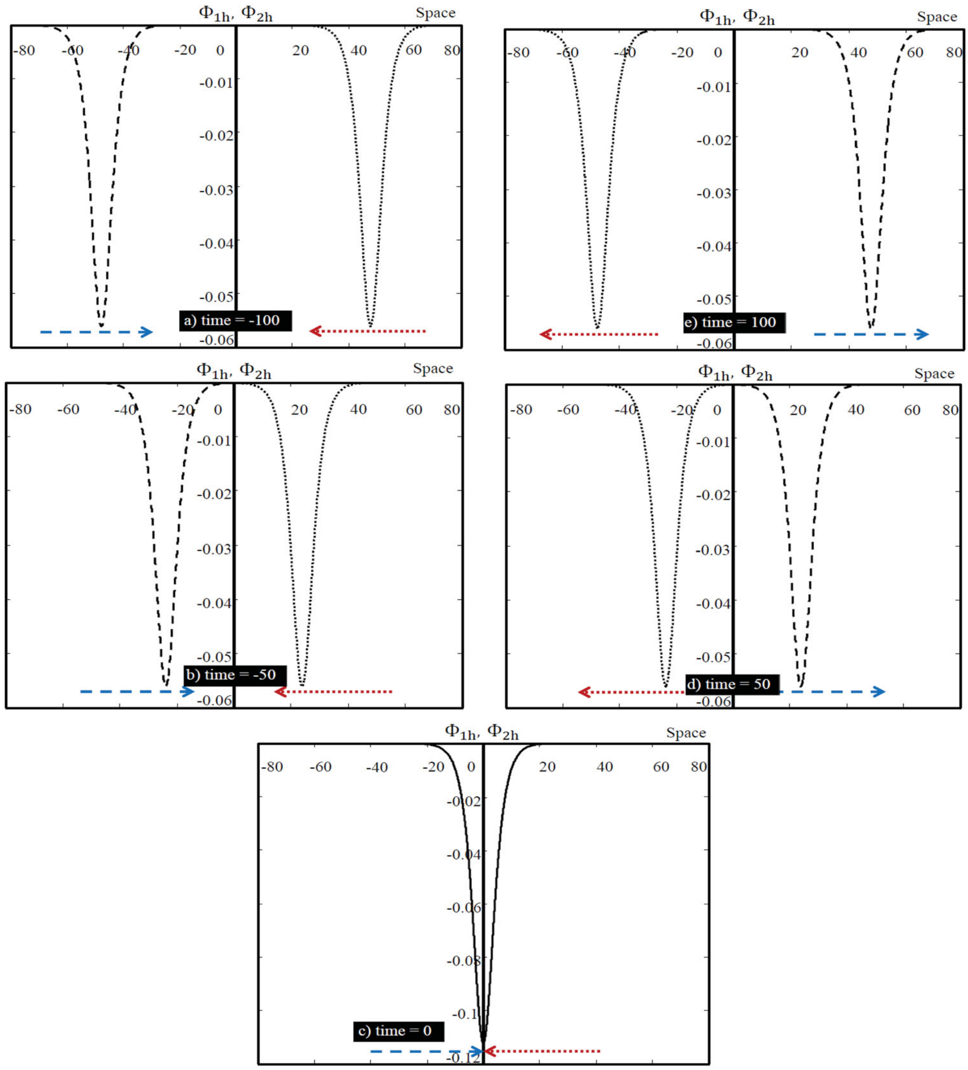

Figure 5. The face-to-face collision profiles between two higher-order electrostatic solitons for GaAs semiconductor at different times.

the exchange–correlation potentials $V_{xce,h}$ on the waveforms of electrostatic solitons. In the presence of $V_{xce,h}$, the amplitude and width of the electrostatic soliton enhance, indicating strong nonlinearity. Figure 4 demonstrates the time evaluation of the face-to-face collision of two electrostatic solitons against space for different times. Initially, two electrostatic solitons are far apart and then go ahead towards each other. As time goes on, they will collide, depart, and then the two electrostatic solitons will regain their original shapes eventually with various phase shifts. As displayed in Figure 4, one can see that the time evaluations of the face-to-face collisions are, respectively, demonstrated by negative (positive) values for the case before (after) collisions. At time $= -100$, two electrostatic solitons are far from each other. At time $= -50$, they will start to collide with each other. At time $= 0$, two electrostatic solitons combine to form a single soliton. At time $= 50$, they will start to separate

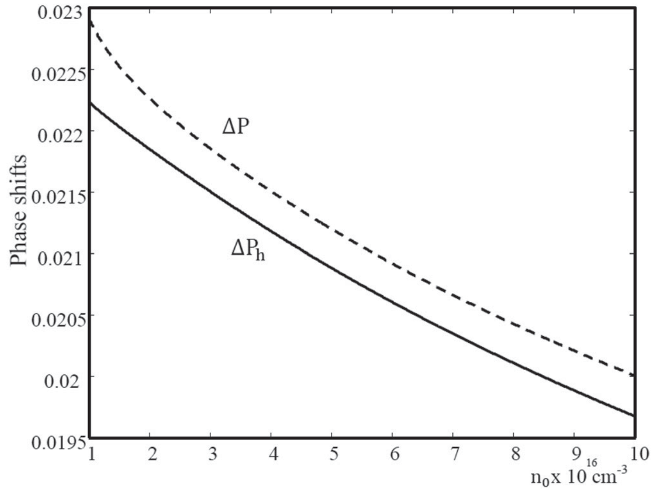

Figure 6. The variation of phase shifts with n_0 for GaAs semiconductor.

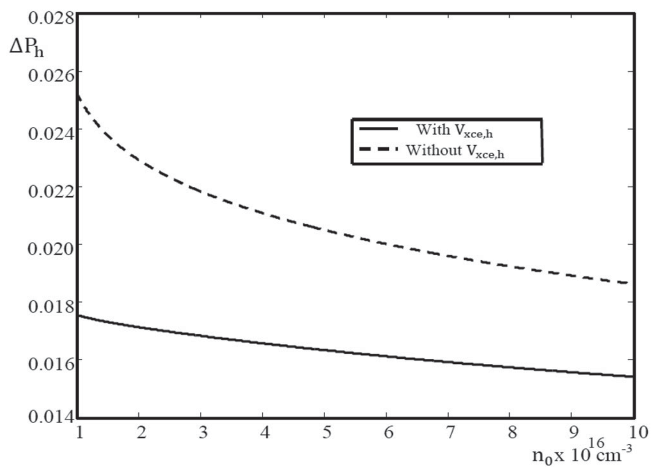

Figure 7. The variation of higher-order phase shift ΔP_h with n_0 for GaAs semiconductor.

from each other. At time = 100, they keep on moving far from each other. Figure 5 illustrates the variation of the time evaluation of the face-to-face collision for two higher-order electrostatic solitons with space for different times. As shown in Figure 5, the collision of two higher-order electrostatic solitons is similar to those in Figure 4. During the collision, an exchange of energies takes place between the two electrostatic solitons, which leads to change in their trajectories (i.e. phase shifts). Now, let us examine the effects of physical parameters, such as n_0 and $V_{xce,h}$, on the phase shifts. Figure 6 exhibits one of the essential results of this study. Figure 6 demonstrates that the phase shifts ΔP and ΔP_h decrease by increasing n_0. Moreover, the higher-order phase shift ΔP_h is smaller than the lowest-order phase shift ΔP. We can say that the large amplitude leads to the short duration of the single

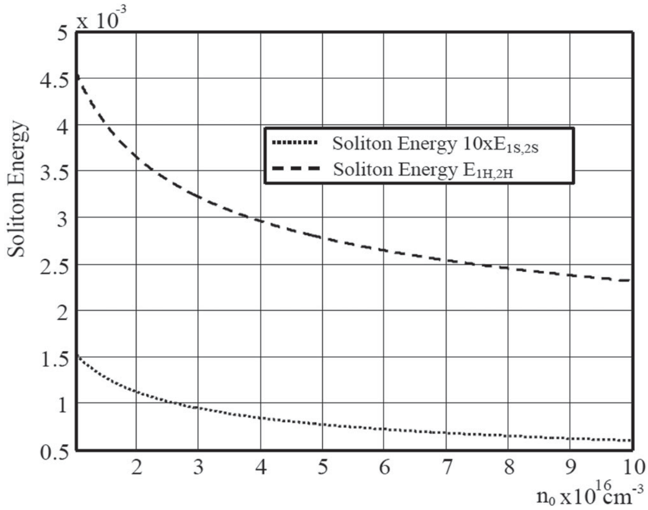

Figure 8. The variation of the soliton energy with n_0 for GaAs semiconductor, the lowest-order soliton energy $E_{1S,2S}$(dotted curve) and the higher-order soliton energy $E_{1H,2H}$ (dashed curve).

peak status, which makes the higher-order phase shift ΔP_h smaller than the phase shift ΔP. Figure 7 reflects the interesting impact of the exchange–correlation potentials $V_{xce,h}$ on the higher order phase shift ΔP_h. It is clear that the presence of $V_{xce,h}$ leads to a decrease in ΔP_h. It is should be mentioned here that the numerical results in Figures 6 and 7 confirm that the numerical results obtained in Figures 1–3 are valid and more powerful. To shed more light on the nature of soliton and its energy, the lowest-order soliton energy $E_{1S,2S}$ and the higher-order electrostatic soliton energy $E_{1H,2H}$ are displayed in Figure 8. In this figure, the soliton energy decreases with an increase in the quantum semiconductor plasma number density n_0. Furthermore, the lowest-order soliton energy gradually decreases with an increase in n_0. On the other hand, there is a critical value of n_0 (i.e. $n_0 < 3 \times 10^{16}\,\text{cm}^{-3}$), where the higher-order soliton energy drastically increases with a slight decrease in the quantum semiconductor plasma number density. Furthermore, if $n_0 > 3 \times 10^{16}\,\text{cm}^{-3}$, the higher-order soliton energy decreases smoothly with an increase in n_0. In general, the unexpected increase in the soliton energy may lead to defects in modern semiconductor devices. Therefore, one can avoid the rapid increase in the soliton energy by adopting a quantum semiconductor plasma number density greater than $3 \times 10^{16}\,\text{cm}^{-3}$ for GaAs. Interestingly, as a distinct point, Figure 8 demonstrates the importance of the higher-order corrections to the nonlinear excitation and collisions of electrostatic solitons. Clearly, we can say that the higher-order soliton energy is highly sensitive and more accurate in comparison to the lowest-order soliton energy. Thus, the sensitive response of the higher-order soliton solutions and their energies indicates that the higher- order corrections play vital roles in a strong understanding of the properties of electrostatic solitons.

In this study, our analysis fundamentally centers on the behavior of electrostatic solitons, their energies and an exchange of energies during the nonlinear propagation and collisions in dens semiconductor plasmas. A theoretical analysis was improved by adding the fifth-order dispersion terms of the KdV equations. In the proposed model, using the plasma parameters for GaAs semiconductors, higher-order solitons are observed to carry energy greater than lowest-order solitons. The results, as shown in Figure 8, confirm that the numerical results obtained in Figures 1 and 6 are more useful and powerful. We believe that the current investigation provides a starting point for further discussion and research in the field of semiconductor plasmas. Finally, due to the effects of higher order corrections, the results give a comprehension view of the understanding of physical scenarios in quantum semiconductors.

Acknowledgments

The authors would like to express their gratitude to the referees for a number of valuable criticisms and comments that have led to improvement of the original manuscript. The authors also thank the editor and his staff for their kind cooperation.

Disclosure statement

No potential conflict of interest was reported by the authors.

Funding

This work was supported by the Deanship of Scientific Research at King Khalid University [Grant Number the project under grant number KKU-G.R.P.-398-39H].

References

[1] Markowich PA, Ringhofer CA, Schmeiser C. Semiconductor equations. New York: Springer-Verlag; 1990.
[2] Ang LK, Kwan TJT, Lau YY. New scaling of Child-Langmuir law in the quantum regime. Phys Rev Lett. 2003;91:208303.
[3] Killian TC. Experiments in botany. Nature (London). 2006;441:298.
[4] Glenzer SH, Landen OL, Neumayer P. Observations of plasmons in warm dense matter. Phys Rev Lett. 2007;98:065002.
[5] Dunne M. A high-power laser fusion facility for Europe. Nature Phys. 2006;2:2.
[6] Wang Y, Shukla PK, Eliasson B. Instability and dynamics of two nonlinearly coupled intense laser beams in a quantum plasma. Phys Plasmas. 2013;20:013103.
[7] Shukla PK, Eliasson B. Novel attractive force between ions in quantum plasmas. Phys Rev Lett. 2012;108:165007.
[8] Zeba I, Yahia ME, Shukla PK, et al. Electron–hole two-stream instability in a quantum semiconductor plasma with exchange-correlation effects. Phys Lett A. 2012;376:2309–2312.
[9] El-Shamy EF, Gohman FS. Propagation and collision of soliton rings in quantum semiconductor plasmas. Phys Lett A. 2014;378:2688–2694.
[10] Choudhury S, Das TK, Ghorui MK, et al. The effect of exchange-correlation coefficient in quantum semiconductor plasma in presence of electron-phonon collision frequency. Phys Plasmas. 2016;23:062110.
[11] Choudhury S, Das TK, Ghorui MK, et al. Propagation and interaction of two soliton in a quantum semiconductor plasma with exchange correlation effects. Phys Plasmas. 2017;24:062103.
[12] Egorov OA, Skryabin DV, Lederer F. Polariton solitons due to saturation of the exciton-photon coupling. Phys Rev B. 2010;82:165326.
[13] Moslem WM, Zeba I, Shukla PK. Solitary acoustic pulses in quantum semiconductor plasmas. Appl Phys Lett. 2012;101:032106.
[14] Wang Y, Lü X. Modulational instability of electrostatic acoustic waves in an electron-hole semiconductor quantum plasma. Phys Plasmas. 2014;21:022107.
[15] El-Bedwehy NA. Freak waves in GaAs semiconductor. Physica B. 2014;442:14–117.

[16] Tolba RE, El-Bedwehy NA, Moslem WM, et al. Nonlinear structures: Cnoidal, soliton, and periodical waves in quantum semiconductor plasma. Phys Plasmas 2016;23:012111.
[17] EL-Shamy EF, Gohman FS, Alqahtani MM, et al. The effects of geometrical configurations on the head collision on nonlinear solitary pulses in a quantum semiconductor plasma: A case study on GaAs semiconductor. Phys Plasmas. 2018;25:012108.
[18] Abdelwahed HG, El-Shewy EK, Zahran MA, et al. The effect of higher-order corrections on the propagation of nonlinear dust-acoustic solitary waves in a dusty plasma with nonthermal ions distribution. Z Naturforsch A. 2008;63:261–273.
[19] Watanabe S, Jiang B. Higher-order solution of an ion-acoustic solitary wave in a plasma. Phys Fluids B. 1993;5:409.
[20] Tiwari RS, Mishra MK. Ion-acoustic dressed solitons in a dusty plasma. Phys Plasmas. 2006;13:062112.
[21] El-Bedwehy NA. Higher-order contribution to dust-ion acoustic dressed solitons in a warm dusty plasma. Phys Plasmas. 2008;15:073709.
[22] El-Labany SK, El-Shamy EF, El-Warraki SA. Dressed ion-acoustic solitons in magnetized dusty plasmas. Phys Plasmas. 2009;16:013703.
[23] El-Labany SK, Shalaby M, El-Shamy EF, et al. Effects of two-temperature electrons, external oblique magnetic field, concentration of charged dust grains and higher-order nonlinearity on dust ion-acoustic solitary waves in Saturn's E-ring. Planet Space Sci. 2009;57:1246–1253.
[24] Kodama Y, Taniuti T. Higher order approximation in the reductive perturbation method. I. the weakly dispersive system. J Phys Soc Jpn. 1978;45:298–310.
[25] Chatterjee P, Das B, Mondal G, et al. Phys. higher-order corrections to dust ion-acoustic soliton in a quantum dusty plasma. Phys Plasmas. 2010;17:103705.
[26] Parveen S, Mahmood S, Adnan M, et al. Characteristic study of head-on collision of dust-ion acoustic solitons of opposite polarity with kappa distributed electrons. Phys Plasmas. 2016;23:092122.
[27] El-Labany SK, El-Shamy EF, El-Bedwehy NA, et al. Nonlinear ion acoustic ring solitons in a multicomponent plasma with superthermal electrons: propagation and collision. Phys Plasmas. 2016;23:102116.
[28] Parveen S, Mahmood S, Qamar A, et al. Interaction of magnetoacoustic solitons in electron-positron plasmas. Adv Space Res. 2019;63:1192–1203.
[29] Abdelwahed HG, El-Shewy EK, Zahran MA, et al. The effect of higher-order corrections on the propagation of nonlinear dust-acoustic solitary waves in a dusty plasma with Nonthermal Ions Distribution. Z Naturforsch. 2008;63a:261–272.
[30] El-Shamy EF, El-Shewy EK, Abdo NF, et al. Dust ion-acoustic solitons collision in weakly relativistic plasmas with superthermality-distributed electrons and positrons: higher-order phase shifts. Contrib Plasma Phys. 2019;59:304–313.
[31] El-Shamy EF. Head-on collision of ion thermal waves in a magnetized pair-ion plasma containing charged dust impurities. Phys Plasmas. 2009;16:113704.
[32] El-Labany SK, El-Shamy EF, Abu El-Eneen M. Head—on collision of nonlinear dust—acoustic solitary waves in dusty plasmas with dust of opposite polarities. Astrophys Space Sci. 2012;337:275–281.
[33] Parveen S, Mahmood S, Qamar A, et al. Interaction of magnetoacoustic solitons in plasmas with dispersion effects through electron inertia. Contrib Plasma Phys. 2018;58:1015–1026.
[34] Parveen S, Mahmood S, Adnan M, et al. Oblique interaction of dust-ion acoustic solitons with Superthermal electrons in a Magnetized plasma. J Phys Soc Jpn. 2018;87:014502.
[35] Epstein M, Johnston CR. Improved solution for solitary waves in arteries. J Math Biol. 1999;39:1–18.
[36] Johnston CR, Epstein M. On the exact amplitude, speed and shape of ion-acoustic waves. Phys Plasmas. 2000;17:906.
[37] Ko K, Kuehl HH. Korteweg-de Vries soliton in a Slowly Varying medium. Phys Rev Lett. 1978;40:233–236.
[38] Kuehl HH, Pereira NR. Energy loss of a modified Korteweg–de Vries solitary wave in a varying medium. Phys Fluids. 1980;23:1471–1472.

[39] Zutavern FJ, Baca AG, Chow WW, et al. Semiconductor lasers from photoconductive switch filaments. Las Vegas: in IEEE Pulsed Power Plasma Science Conference; 2001.

Appendix

The equations depending on the order of ε are given

$$\varepsilon^0 : -\Lambda_0 \frac{d\Phi_{01}}{d\Xi} + A\Phi_{01}\frac{d\Phi_{01}}{d\Xi} + B\frac{d^3\Phi_{01}}{d\Xi^3} = 0,$$

$$\varepsilon^0 : -\Lambda_0 \frac{d\Phi_{02}}{dZ} + A\Phi_{02}\frac{d\Phi_{02}}{dZ} + B\frac{d^3\Phi_{02}}{dZ^3} = 0,$$

$$\varepsilon^1 : L_\Xi\Phi_{11} = \Lambda_1\frac{d\Phi_{01}}{d\Xi} - \frac{d^5\Phi_{01}}{d\Xi^5},$$

$$\varepsilon^1 : L_Z\Phi_{12} = \Lambda_1\frac{d\Phi_{02}}{dZ} - \frac{d^5\Phi_{02}}{dZ^5},$$

$$\varepsilon^2 : L_\Xi\Phi_{21} = \Lambda_1\frac{d\Phi_{11}}{d\Xi} + \Lambda_2\frac{d\Phi_{01}}{d\Xi} - A\Phi_{11}\frac{d\Phi_{11}}{d\Xi} - \frac{d^5\Phi_{11}}{d\Xi^5},$$

$$\varepsilon^2 : L_Z\Phi_{22} = \Lambda_1\frac{d\Phi_{12}}{dZ} + \Lambda_2\frac{d\Phi_{02}}{dZ} - A\Phi_{12}\frac{d\Phi_{12}}{dZ} - \frac{d^5\Phi_{12}}{dZ^5},$$